Research Article

Dependence of MeV TOF SIMS secondary molecular ion yield from phthalocyanine blue on primary ion stopping power

Marko Brajkovic, Marko Barac, Iva Bogdanovi# Radovi#, and Zdravko Siketic

J. Am. Soc. Mass Spectrom., **Just Accepted Manuscript** • DOI: 10.1021/jasms.0c00080 • Publication Date (Web): 26 May 2020

Dependence of MeV TOF SIMS secondary molecular ion yield from phthalocyanine blue on primary ion stopping power

Marko Brajković, Marko Barac, Iva Bogdanović Radović, Zdravko Siketić*

Ruđer Bošković Institute, Bijenička c. 54, HR-10000 Zagreb, Croatia

*corresponding author, zsiketic@irb.hr

Keywords: MeV TOF SIMS, secondary ion yield, phthalocyanine blue, electronic stopping, primary ion charge state

Address reprint requests to:

Zdravko Siketić, Bijenička c. 54, 10000 Zagreb, Croatia, +38514571227, zsiketic@irb.hr

Abstract

Time-of-flight Secondary Ion Mass Spectrometry (TOF SIMS) is a well-established mass spectrometry technique used for the chemical analysis of both organic and inorganic materials. In the last ten years, many advances have been made to improve the yield of secondary molecular ions, especially those desorbed from the surfaces of organic samples. For that, cluster ion beams with keV energies for the excitation were mostly used. Alternatively, single-ion beams with MeV energies can be applied, as done in the present work. It is well known that secondary molecular/ion yield depends strongly on the primary ion stopping power, but the nature of this dependence is not completely clear. Therefore, in the present work secondary ion yield from the phthalocyanine blue ($C_{32}H_{16}CuN_8$, organic pigment) was measured for the various combinations of ion masses, energies and charge states. Measured values were compared with the existing models for ion sputtering. An increase of the secondary yield with the primary ion energy, electronic stopping, velocity and charge state was found for different types of primary ions. Although this general behavior is valid for all primary ions, there is no single parameter that can describe the measured results for all primary ions at once.

Introduction

Time-of-flight secondary ion mass spectrometry (TOF SIMS) using a primary ion beam in the MeV energy range has two main advantages compared to conventional keV SIMS: several orders of magnitude higher secondary molecular ion yield of desorbed heavier molecules and less fragmentation [1,2]. This increases detection sensitivity for heavier molecules which is particularly important for molecular imaging and facilitates analysis and interpretation of mass spectra. It is well known that the interaction mechanism between incident MeV ion and molecules at the sample surface is the main reason for the above-mentioned difference. Nuclear collisions that dominate in the interaction of keV single primary ions with the target atoms are negligible compared to the electronic excitation in the case of MeV ions [2,3]. Theoretical description of this electronic sputtering which results in the desorption of intact molecules is not easy and, although several models are proposed, such as the thermal spike model [4,5], pressure pulse model [6] or popcorn model [7], there is still no model which can reliably predict molecular yield for a wide energy range of different primary ions and targets. Models [6] and experiments [8] show cubic dependence for sputtering yield of neutral particles as a function of primary ion electronic stopping power, but for molecular ions, where ionization mechanism is critically important, dependence is not clear. Some models (i.e. thermal spike model) and experimental results suggest quadratic dependence for the yield as a function of electronic stopping [8,9], while some experimental results show that stronger dependence can be expected [8,9,10], up to the forth power. Previous experiments also showed sample dependence of molecular ion yield [10].

In the present work, the secondary molecular yields of copper(II) phthalocyanine (also known as phthalocyanine blue), a synthetic organic blue pigment frequently used in paints and dyes, for several primary ions with different energies and charge states have been measured. The dependence of the obtained molecular yields on primary ion electronic stopping, velocity and charge state was compared with the predictions of existing theoretical models.

Experimental setup and procedure

Different primary ions (Cl, Si, Fe, Cu, I and Au) with several charge states and energies from 3.37 MeV up to 20.2 MeV were obtained using a 6 MV Van de Graaff accelerator. Measurements were performed at the recently finished setup for MeV TOF SIMS which uses a glass capillary for primary beam collimation and a TOF reflectron for mass analysis [11]. The sample, a phthalocyanine blue ($C_{32}H_{16}CuN_8$, m = 576.082 Da) evaporated on a 100 nm thick Si_3N_4 window, was placed in the vacuum chamber (working pressure ~ $1 \cdot 10^{-7}$ hPa) on a scanning piezo stage mounted in front of the capillary tip. Primary ions pass through the sample and hit a Hamamatsu S3590-09 silicon PIN diode placed 10 mm behind the target which triggers the START signal for the time-of-flight measurements. A PIN diode is mounted on the scanning stage and moves together with the sample. This allows different positions on the detector to be hit by the primary ions, reducing irradiation-induced deterioration of the diode's properties. No change in timing/mass resolution of collected spectra was observed during the measurements. Positive secondary ions were collected in a dual slope TOF reflectron analyzer with a MCP detector. The reflectron analyzer corrects for the initial energy distribution of secondary ions to the first order and thus has supreme mass resolution when compared to a linear TOF analyzer. The target voltage was set to +4.5 kV. Details about the reflectron voltages can be found in [11]. The time resolution of the SIMS spectra was around 5 ns for hydrogen (m/q = 1). This corresponds to a mass resolution of around 1800 for m/q = 576 Da. The coincidence window, time between the impact of primary ion and detection of secondary ions, was set to 100 µs.

Secondary molecular ion yield is defined as the ratio of the number of detected secondary ions for selected mass (calculated as an area under the selected peak in the mass spectrum) to the number of primary ions hitting the sample (events detected by particle detector). To minimize the effects of different sample surface conditions and geometry to the measured secondary molecular yields, spectra were collected from the same scanned area on only one sample. The primary beam was collimated using a borosilicate capillary with an exit diameter of 2.5 microns. Beam halo, a result of

scattering of the primary ions near the capillary tip, together with beam divergence due to imperfect beam optics, reduces the lateral resolution at the sample surface to about 5 x 10 μm^2, independent of the primary ion type and energy. The predefined scan size was set to 250 x 250 μm^2 with a 5 µm pixel size, but the real scan size was smaller. Acquisition of each spectrum was stopped when about 1000 counts were recorded in the peaks of interest (m/q = 575-578 Da). At this scale, no surface inhomogeneity was observed. Primary beam currents, measured by PIN diode, were 150-800 Hz depending on the primary ion type and energy. The cumulative fluence for all measurements was around $5 \cdot 10^{10}$ ions/cm^2, at least an order of magnitude less than the static limit of SIMS (around 10^{12} ions/cm^2), so the variation of molecular yield due to surface damage can be neglected.

Results and discussion

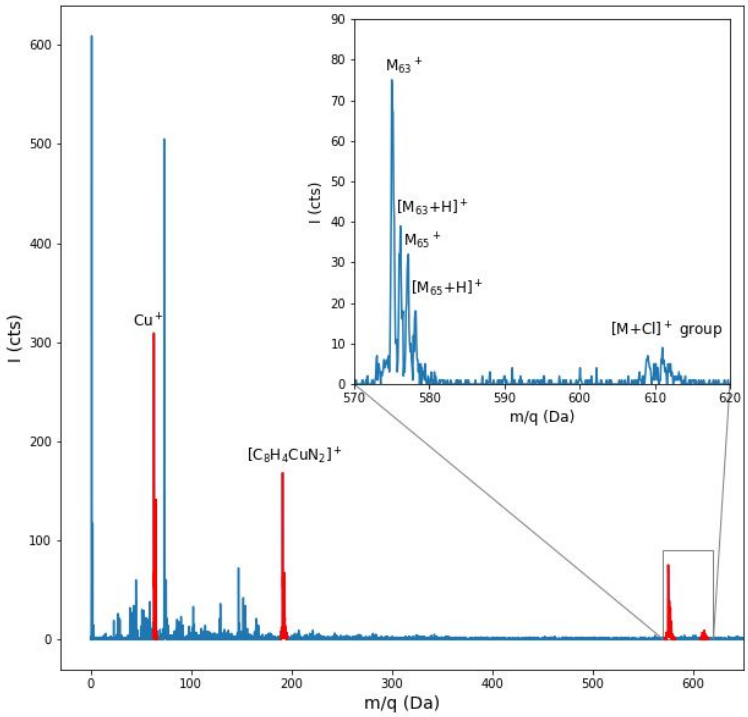

Fig. 1 TOF-SIMS spectrum of phthalocyanine blue. The primary ion is 20 MeV I^{6+}. The main molecular peak and its fragments are colored in red. Main molecular peaks $[M]^+$ with mass m/q = 575 Da (with ^{63}Cu isotope) and m/q = 577 Da (with ^{65}Cu isotope) are shown in the figure inset.

A typical measured mass spectrum of copper phthalocyanine is shown in Figure 1. Main molecular peaks $[M]^+$ with mass m/q = 575 Da (with ^{63}Cu isotope) and m/q = 577 Da (with ^{65}Cu isotope) are shown in the figure inset. They are associated with peaks of protonated phthalocyanine molecules (m/q = 576 and m/q =578, for two Cu isotopes). There is also a group of peaks from m/q = 609 Da to m/q = 612 Da, which is a signature of chlorine stabilized PB15 pigment (called PB15:1) containing 0.5 – 1 Cl atoms per molecule (1 H atom from the phthalocyanine ring is substituted by Cl atom which leads to the mass difference of 34). Since the yield of this group of peaks is very low, it was not used in the analysis. Additionally, the mass spectra phthalocyanine fragment ions $[C_8H_4CuN_2]^+$ at m/q = 191 Da (with ^{63}Cu isotope) and m/q = 193 Da (with ^{63}Cu isotope) are present, as well as two Cu isotopes. The ratio of the measured yields of the two stable copper isotopes ^{63}Cu and ^{65}Cu (2.28 ± 0.10) is in accordance with their natural abundances (69.15% : 30.85%). The other intensive peaks (m/q = 73, 147, 207, 221) belong to PDMS (polydimethylsiloxane), a well-known and often present surface contaminant.

To calculate yields of different ions, spectrum background has to be subtracted. In our case that was 2-3% of the counts present in the main molecular peak. This is a result of false stop signals when a new primary ion (from the primary beam core or halo) hits the sample during the acquisition window triggered by the previous one. In that case, new stop signals will arrive in the MCP detector which are uncorrelated with the previous start signal and therefore cause random events in the spectrum. In order to minimize this effect, relatively low primary currents were used (below 1 kHz at the sample for 100 μs acquisition window).

Concerning the molecular fragments, the yield of the secondary molecular ions depends on fundamental parameters (sputtering yield and ionization probability), but also on the system detection efficiency. Therefore, the Einzel lens voltage (2.33 kV) was optimized to maximize secondary ion collection. It is known that the MCP efficiency in this range of acceleration voltage (4.5 kV) depends on the ion velocity: for the same number of sputtered ions, a smaller number of slower ones (heavier)

will be detected. Since the MCP efficiency as a function of ion velocity was not measured, no conclusions can be drawn on the yield difference between fragments and whole molecular ions for one mass spectrum. Therefore, the same mass peaks were compared for various types and energies of primary ions.

Total secondary molecular ion yield, calculated as the number of all detected secondary ions (minus background) per one primary ion, was in the range of 3 – 9%, depending on the primary ion properties and was almost an order of magnitude lower than the total molecular yield measured using a simple linear TOF analyzer [12,13]. As expected, 5 – 10 times better mass resolution for the reflectron TOF analyzer comes at the expense of a similar decrease in the detection efficiency [14].

Molecular yields of phthalocyanine blue (from m/q = 575 to m/q = 578) for various primary ions are shown in Table 1 and Figure 2.

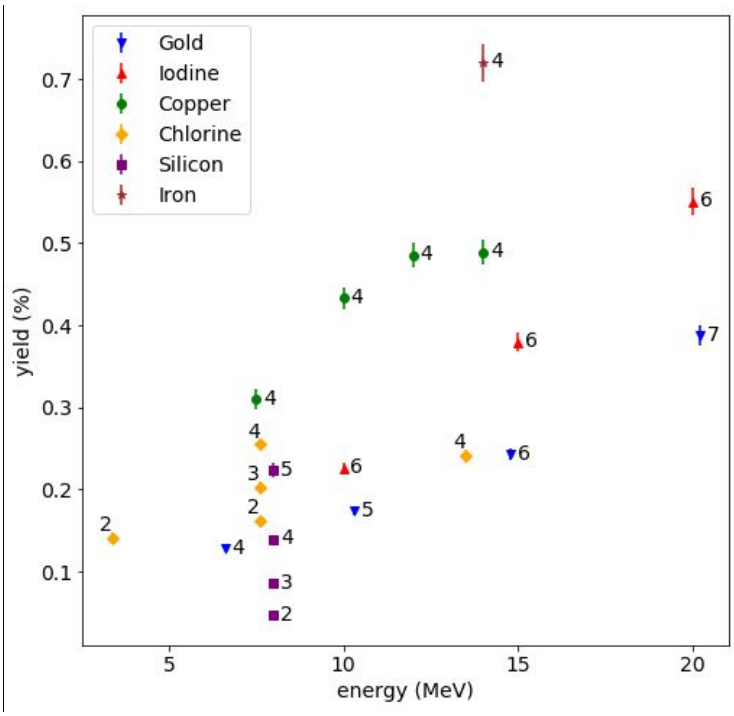

Fig. 2 Yield of the phthalocyanine blue main molecular peak (m/q = 575-578 Da) as a function of primary ion energy. The charge state of the primary ion is written next to each data point.

Table. 1 Molecular yield for different primary ion types, energies and charge states. Electronic stopping values are calculated using software CasP [16], while nuclear stoppings are calculated using SRIM [15].

ion	charge state	energy (MeV)	velocity/c	dE/dx-el. (eV/A)	dE/dx-nucl. (eV/A)	Yield (%), m/q = 575-578 Da	Yield (%), m/q = 191-194 Da
Au	4	6.6	0.008	111.96	116.64	0.128	0.250
Au	5	10.3	0.011	166.08	90.90	0.174	0.308
Au	6	14.8	0.013	226.52	72.85	0.243	0.417
Au	7	20.2	0.015	292.72	59.55	0.388	0.608
I	6	20	0.018	326.92	22.49	0.551	0.906
I	6	15	0.016	282.39	27.67	0.379	0.650
I	6	10	0.013	218.40	36.66	0.226	0.402
Si	5	8	0.025	212.47	1.30	0.224	0.337
Si	4	8	0.025	185.89	1.30	0.139	0.215
Si	3	8	0.025	163.22	1.30	0.085	0.132
Si	2	8	0.025	144.72	1.30	0.047	0.071
Cu	4	14	0.022	222.12	5.98	0.489	0.661
Cu	4	12	0.020	209.09	6.74	0.485	0.643
Cu	4	10	0.018	195.54	7.76	0.433	0.606
Cu	4	7.5	0.016	178.27	9.65	0.310	0.453
Fe	4	14	0.023	245.65	4.49	0.720	0.883
Cl	2	7.6	0.022	166.49	2.31	0.162	0.279
Cl	3	7.6	0.022	183.52	2.31	0.203	0.289
Cl	4	7.6	0.022	204.35	2.31	0.255	0.365
Cl	2	3.37	0.014	120.80	4.37	0.141	0.242
Cl	4	13.5	0.029	207.90	1.46	0.241	0.336

Absolute values of molecular yields, from the lowest yield of 0.05% for 8 MeV Si^{2+} to the highest yield of 0.72% for 14 MeV Fe^{4+}, are in the expected range, which is about an order of magnitude lower than the total yield [12]. From Figure 2, it can be concluded that secondary molecular yield is increasing with increasing primary ion energy for all ions. For Cu, Fe, I and Au ions, the molecular yield is higher for lighter ions over the whole energy range shown. Also, concerning the primary ion charge state, a higher yield was measured for a higher charge state of ions having the same energy.

To compare yield dependence with the electronic stopping of the primary ions, theoretical stopping power values are required. For that purpose, values calculated by SRIM [15] were not used because

SRIM gives stopping values for equilibrium ion charge state in the material which is determined by the balance between electron capture and projectile-electron loss, a function of projectile's velocity and projectile and target atomic numbers. This mean charge, however, is reached after traveling tens of nm in the target, which is a larger depth than the ejection depth of the desorbed molecules (uppermost layers of the target). Also, SRIM stopping calculation for the measured energy region (50 – 300 keV/u), slightly below the Bragg peak, is known to have relatively large deviations (up to 20%) from experimental results [16]. Therefore, the CasP program was used (with program parameters: UCA model, DHFS screening potential) to calculate electronic stopping since it provides non-equilibrium energy loss and takes the charge state of the incident ion into account [16]. Figure 3 shows that molecular yield is increasing with the electronic stopping of the primary ion. If we assume a scaling of the yield with the power of electronic stopping, its magnitude is, as it can be seen, not the same for all primary ions. To access the range of parameters that describe the data, three subsets (see Figure 3) that show a similar dependence on electronic stopping have been recognized and separately analyzed. Parameters of the power functions for each subset were extracted by applying the least square fit to log(y)-log(x) data. Copper shows stronger dependence (power of 2.4) than Au, I and Cl ions (power of 1.31), while Si ions have even higher dependence (power of 4). The first two subsets do not show dependence predicted by some of the models (quadratic or fourth power) [4,5,6,9,10]. On the other hand, similar behavior to the silicon data can be found in previous results [8,9,10]. Deviations from the stopping dependence for neutrals [6,8] confirm that the ionization part of the desorption process plays an important role in molecular ion yield. The obtained results should not be taken as a pass-fail test of the above-mentioned models given the limitations of this analysis, such as certain arbitrariness in the subsets choice, the sensitivity of the power fits to single data points, neglect of the charge exchange processes that affect calculated stopping power at the very surface of the sample, and limited velocity range.

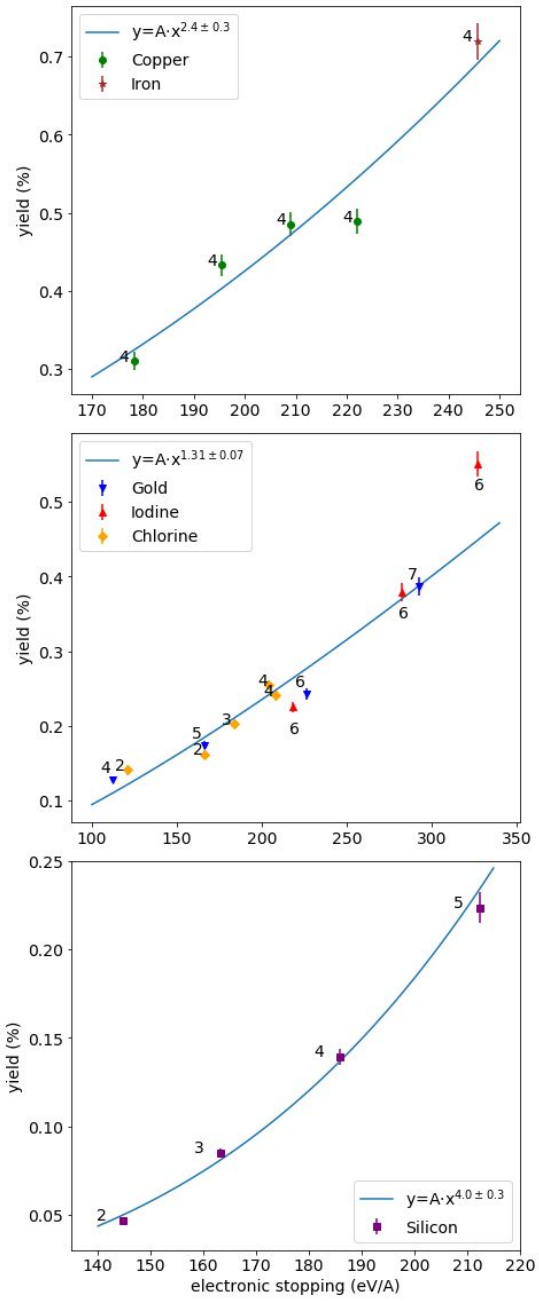

Fig. 3 The yield of the phthalocyanine blue main molecular peak (m/q = 575-578 Da) as a function of the electronic stopping of the primary ion (calculated using CasP [16]). The charge state of the primary ion is written next to each data point. The best fit is shown for each data set.

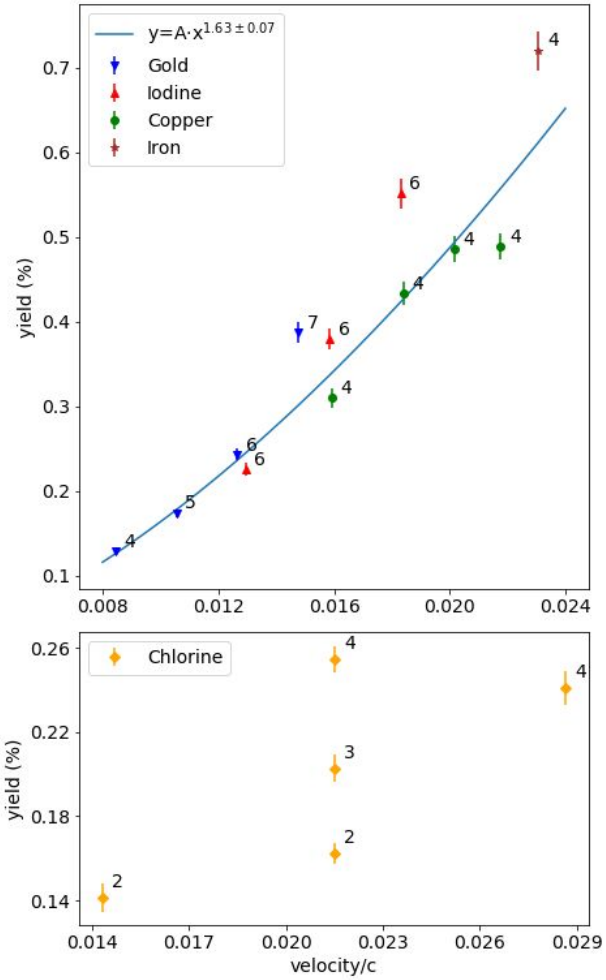

Fig. 4 Yield of the phthalocyanine blue main molecular peak (m/q = 575-578 Da) as a function of primary ion velocity. The charge state of the primary ion is written next to each data point. The best fit is shown for the first data set.

Velocity dependence of the yield is shown in Figure 4. When comparing the yield for Cu, Fe, I and Au, it can be concluded that ion velocity is a better predictor than its stopping power: in the same range of electronic stopping Cu and Fe produce a higher molecular yield than I and Au, but the difference disappears when looking at the yield as a function of primary ion velocity. For chlorine ions, on the other hand, velocity (or energy) has almost no effect on the secondary ion yield whose rise is perfectly

correlated with the charge state of chlorine ion. It can also be seen that for roughly the same velocity, yield increases with an increase in electronic stopping (7.6 MeV Cl^{2+} vs 20.2 MeV Au^{7+}, 7.5/10 MeVCu^{4+} vs 15/20 MeV I^{6+}, 7.6 MeV Cl^{4+} vs 14 MeV Cu^{4+} and 14 MeV Fe^{4+}, see Figures 3 and 4 and Table 1). These results can be qualitatively explained taking into account the ion track model which assumes two energy deposition cylindrically-shaped regions [17]: one close to the ion track characterized by the primary excitations and ionization (called infratrack) and a second and larger region (called ultratrack) where secondary electrons created in the infratracks deposit energy and by some means (through bond breaking [10] or exciting of vibrational modes of molecules [7], depending on the model) cause desorption of the molecules. In this model, where ultratrack radii are defined by primary ion velocities and deposited energy by its electronic stopping, the desorption yield of the molecules is determined by the density of the deposited energy. For the same velocity, a higher stopping ion will deposit a larger amount of energy in the same volume causing a larger deposited energy density resulting in a higher desorption yield which is in accordance with our experimental results. While this model predicts a higher yield for slower ions for same electronic stopping, experimental results are inconclusive – it cannot be said whether slower (8 MeV Si^{3+} vs 7.6 MeV Cl^{2+} vs 10.3 MeV Au^{5+}, 8 MeV Si^{5+} vs 12 MeV Cu^{4+}) or faster ions (10 MeV I^{6+} vs 14 MeV Cu^{4+}) produce a higher yield.

The molecular yield as a function of the primary ion charge state is shown in Figure 5 for 7.6 MeV Cl and 8 MeV Si. Yield increases almost linearly with the charge state for chlorine and stronger for silicon, but there is not enough data to draw hard conclusions. It would be useful to have data for more highly charged ions, since some experiments with slow highly charged ions showed a transfer of potential energy to the surface electrons through the charge exchange processes as a major contribution to secondary ion sputtering [18]. Previous experiments with MeV ions showed dependence on roughly the fourth power of charge state for a charge state greater than 6 [19]. However, the primary beam current for these highly charged states was too low in our case to perform a measurement.

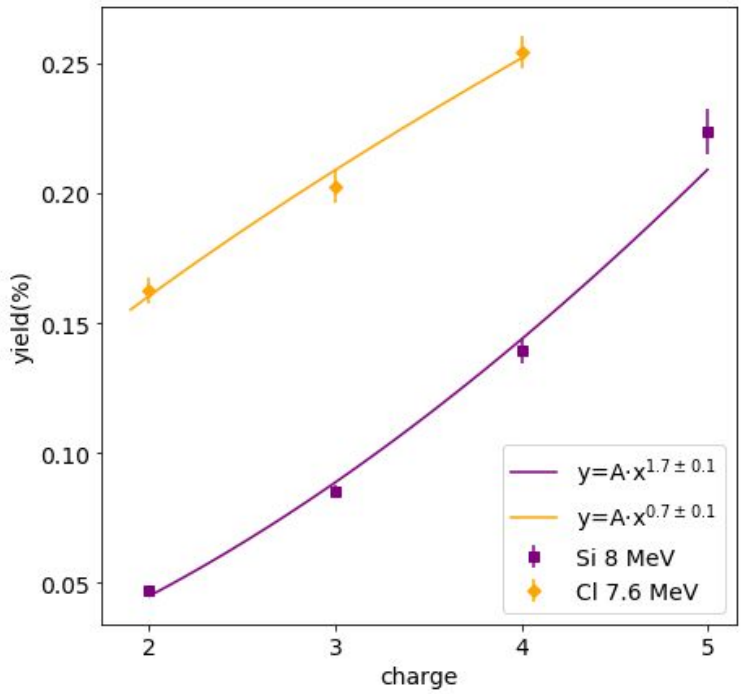

Fig. 5 Yield of phthalocyanine blue main molecular peak (m/q = 575-578 Da) as a function of the primary ion charge state. The best fit is shown for both ions.

Yield dependence of phthalocyanine fragment (m/q = 191-194 Da) as a function of electronic stopping of the primary ion is shown in Figure 6. Almost identical behavior as the full molecular ion is measured for the fragment ion. At the same time, the ratio between fragment yield and main molecular ion yield increases with the ratio of the nuclear and electronic stopping power of the primary ions (Figure 7), but as the stopping ratio increases over 50 times, the yield ratio increases less than 2 times, which means that in this energy region the same mechanism drives desorption of intact molecules and a large majority of molecular fragments. Data for Si and Cl ions are not displayed since all Si ions and three out of five Cl ions have the same comparatively small nuclear stopping.

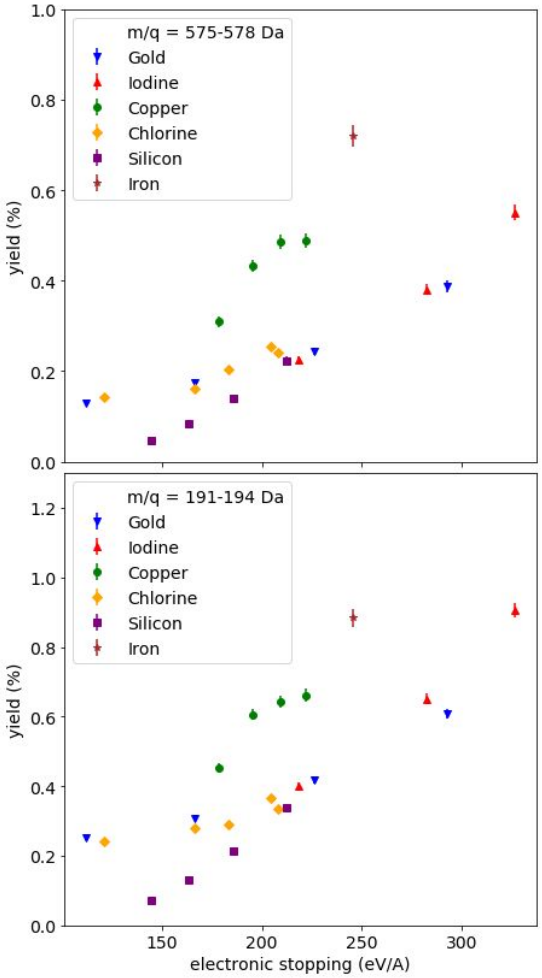

Fig. 6 Comparison of yield of the phthalocyanine blue main molecular peak (m/q = 575-578 Da) and its fragment (m/q = 191-194 Da) as a function of electronic stopping of the primary ion (calculated using CasP [16]).

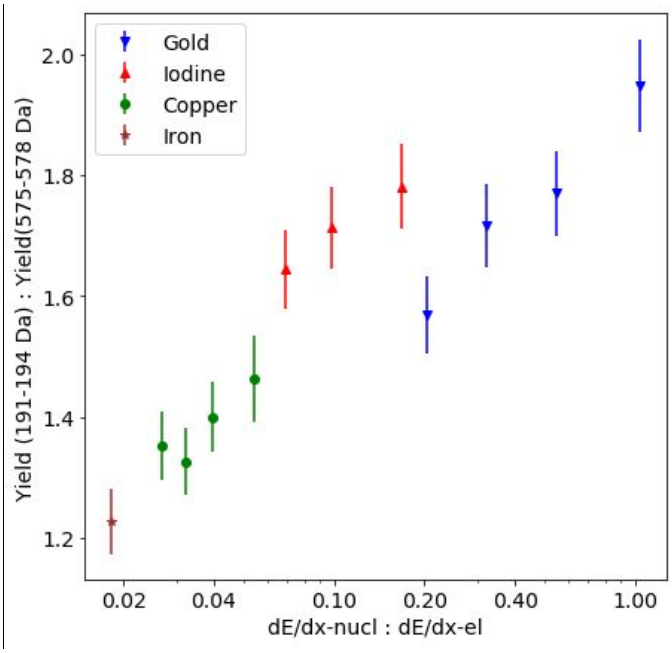

Fig. 7 The yield ratio of the fragment (m/q = 191-194 Da) and the main molecular peak (m/q = 575-578 Da) for phthalocyanine blue as a function of the ratio of nuclear and electronic stopping of the primary ion. Nuclear stopping is calculated using SRIM [15] and electronic stopping is calculated using CasP [16].

Conclusion

Measured molecular yields of phthalocyanine blue for different primary ions show a positive correlation to primary ion energy, electronic stopping, velocity and charge state. Although this general behavior is valid for all primary ions, there is no single parameter that can describe the measured results for all ions at once. Inadequate models that do not pay attention to the ionization but are concentrated on the sputtering part of the desorption process cannot quantitatively describe measured results, but the latter in principle agree partly with the prediction of the ion track model. This model shows linear behavior of the molecular yield in higher electronic stopping region, but due to the limitations of the used accelerator, these higher energies could not be accessed. To choose the optimum primary ion, both its velocity and electronic stopping must be considered – in our case the best primary ion is 14 MeV Fe^{4+}, although it does not have the highest velocity (13.5 MeV Cl^{4+}, but with a low stopping power compared to Fe) nor the highest stopping power (20 MeV I^{6+}, but slower than

Fe). One must obviously find a delicate balance on the higher end of the available values for these two quantities.

The relatively low molecular yield with the used experimental setup (less than 1%), primarily constrained by the TOF reflectron analyzer, is a serious obstacle in utilizing it for imaging of biological molecules. One possible improvement is background minimization by reducing the false start and stop signals with the installation of a beam deflector prior to the capillary microprobe chamber. In this way, during the acquisition window for TOF measurements, no new primary ion should arrive on the sample and create false events. With this upgrade, even with relatively low molecular yield, heavy molecular ion peak formation and relevant statistics should be accessible in a reasonable timeframe.

Acknowledgments

M. Brajković acknowledges support by the Croatian Science Foundation (CSF) project "Young Researchers' Career Development Project - Training of Doctoral Students" co-financed by the European Union, Operational Program "Efficient Human Resources 2014-2020" and the ESF. I. B. R. and Z. S. acknowledge support by the CSF project IP-2016-06-1698 "Development of a capillary microprobe for MeV SIMS for analysis of biological materials– BioCapSIMS", by the RADIATE project under the Grant Agreement 824096 from the EU Research and Innovation program HORIZON 2020 and by the Croatian Centre of Excellence for Advanced Materials and Sensing devices research unit Ion Beam Physics and Technology, Ruđer Bošković Institute, Zagreb, Croatia. The authors also wish to thank Dr. Max Döbeli and Dr. Klaus-Ulrich Miltenberger from ETH Zürich for help with micro-capillary production.

References

1. Kamensky, I.; Hakansson, P.; Sundqvist, B.; McNeal, C.J.; Macfarlane, R. Comparison of biomolecule desorption yields for low and high energy primary ions. *Nucl. Instum. Methods Phys. Res.* **1982***, 198,* 65-58.

2. Nakata, Y.; Honda Y.; Ninomiya, S.; Seki, T.; Aoki, T.; Matsuo, J. Yield enhancement of molecular ions with MeV ion-induced electronic excitation. *Appl. Surf. Sci*. **2008**, *255*, 1591-1594.
3. Nakata, Y.; Honda, Y.; Ninomiya, S.; Seki, T.; Aoki, T.; Matsuo, J. Matrix-free high-resolution imaging mass spectrometry with high-energy ion projectiles. *J. Mass. Spectrom*. **2009**, *44*, 128–136.
4. NoorBatcha I., Lucchese R.R. Thermal spike model for heavy ion induced desorption. *PDMS and Cluster. Lecture Notes in Physics*. **1987**, *269*, 81-93.
5. Johnson, R.E. Mechanisms for the desorption of large organic molecules. *Int. J. Mass Spectrom. Ion Processes* **1987**, *78*, 357-392.
6. Johnson, R.E.; Sundqvist, B.U.R.; Hedin, A.; Fenyo, D. Sputtering by fast ions based on a sum of impulses. *Phys. Rev. B* **1989**, *40 (1)*, 49-53.
7. Williams, P.; Sundqvist, B. Mechanism of Sputtering of Large Biomolecules by Impact of Highly Ionizing Particles. *Phys. Rev. Lett.* **1987**, *58 (10)*, 1031-1034.
8. Hedin, A.; Hakansson, P.; Salehpour M.; Sundqvist, B.U.R. Fast-ion-induced erosion of leucine as a function of the electronic stopping power. *Phys. Rev. B* **1987**, *35 (14)*, 7377-7381.
9. Hakansson, P.; Sundqvist, B. The velocity dependence of fast heavy-ion induced desorption of biomolecules. *Radiat. Eff.* **1982**, *61*, 179-193.
10. Hedin, A.; Hakansson, P.; Sundqvist, B. Ion-track model for fast-ion-induced desorption of molecules. *Phys. Rev. B* **1985**, *31 (4)*, 1780-1787.
11. Brajković, M.; Barac, M.; Cosic, D.; Bogdanović Radović, I.; Siketić, Z. Development of MeV TOF-SIMS capillary microprobe at the Ruđer Bošković Institute in Zagreb. *Nucl. Instum. Methods Phys. Res., Sect. B* **2019**, *461*, 247-242.
12. Jenčič, B.; Vavpetič, P.; Kelemen, M.; Pelicon, P. Secondary ion yield and fragmentation of biological molecules by employing ^{35}Cl primary ions within the MeV energy domain. *J. Am. Soc. Mass Spectrom.* **2020**, *31*, 117-123.

13. Stoytschew, V.; Bogdanović Radović, I.; Demarche, J.; Jakšić, M.; Matjačić, L.; Siketić, Z.; Webb, R. MeV-SIMS yield measurements using a Si-PIN diode as a primary ion current counter. *Nucl. Instum. Methods Phys. Res., Sect. B* **2016**, *371*, 194-198.

14. Cotter, R.J. *Time-of-flight mass spectrometry: instrumentation and applications in biological research (ACS Professional Reference Book)*, 1st ed., American Chemical Society, Washington DC, US, 1997.

15. Ziegler, J.F.; Ziegler, M.D.; Biersack, J.P. SRIM – The stopping and range of ions in matter (2010). *Nucl. Instum. Methods Phys. Res., Sect. B* **2010**, *268*, 1818-1823.

16. Grande, P.L.; Schiwietz, G. The unitary convolution approximation for heavy ions. *Nucl. Instum. Methods Phys. Res., Sect. B* **2002**, *195*, 55-63.

17. Pereira, J.A.M.; da Silveira, E.F. Cluster and Velocity Effects on Yields and Kinetic Energy Distributions of Li^+ Desorbed from LiF. *Phys. Rev. Lett.* **2000**, *84 (25)*, 5904-5907.

18. Kakutani, N.; Azuma, T.; Yamazaki, Y.; Komaki, K.; Kuroki, K. Strong charge state dependence of H^+ and H_2^+ sputtering induced by slow highly charged ions. *Nucl. Instum. Methods Phys. Res., Sect. B* **1995**, *96*, 541-544.

19. Hakansson, P.; Jayasinghe E.; Johansson A.; Kamensky, I.; Sudqvist, B. Charge-State Dependence of Desorption of Biomolecules Induced by Fast Heavy Ions, *Phys. Rev. Lett.* **1981**, *47 (17)*, 1227-1229

For Table of Contents Use Only

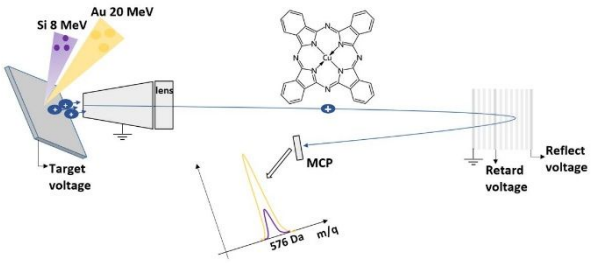

Manuscript title: Dependence of MeV TOF SIMS secondary molecular ion yield from phthalocyanine blue on primary ion stopping power

Authors: Marko Brajković, Marko Barac, Iva Bogdanović Radović, Zdravko Siketić

Description of graphic: Molecular yields of phthalocyanine blue are measured using a reflectron time-of-flight analyzer for different primary ions in the MeV energy region. When comparing results for 8 MeV Si and 20 MeV Au, secondary ion yield is higher for the primary ion with larger electronic stopping (Au 20 MeV).